JPE 14-2-6

http://dx.doi.org/10.6113/JPE.2014.14.2.257
ISSN(Print): 1598-2092 / ISSN(Online): 2093-4718

Highly AC Voltage Fluctuation-Resistant LED Driver with Sinusoid-Like Reference

Ning Ning†, Zhenxiao Tong*, Dejun Yu*, Shuangyi Wu*, Wenbin Chen*, and Chunyi Feng*

†*State Key Laboratory of Electronic Thin Film and Integrated Device,
University of Electronic Science and Technology of China, Chengdu, China

Abstract

A novel converter-free AC LED driver that is highly resistant to the fluctuation of AC voltage is proposed in this study. By removing large passive components, such as the bulky capacitor and the large-value inductor, the integration of the driver circuit is enhanced while the driving current remains stable. The proposed circuit provides LED lamps with a driving current that can follow the sinusoid waveform to obtain a very high power factor (PF) and low total harmonic distortion (THD). The LED input current produced by this driving current is insensitive to fluctuations in the AC voltage. Users will thus not feel that LED lamps are flashing during the fluctuation. Experiment results indicate that the proposed system can obtain PF of 0.999 and THD as low as 3.3% for a five-string 6 W LED load under 220 V at 50 Hz.

Keywords: AC LED, Fluctuation in AC voltage, Sinusoid waveform, power factor (PF), Total harmonic distortion (THD)

I. INTRODUCTION

LED is a photoelectric conversion element with high conversion efficiency. Given the absence of lamp filaments, this pure semiconductor luminous element has a long service life and functions as an environmentally friendly light source. With these advantages, LED has been widely used in various fields, including displays, decorations, backlights, general lighting, and urban landscape lighting [1]-[6].

LED current determines the luminous flux output. Designing a highly reliable and efficient LED driving current is thus very important. AC–DC and DC–DC LED driving circuits [7]-[16] are widely utilized in LED lighting systems. They will also be inevitably applied to AC–DC or DC–DC converters; this condition means that large-value inductors and large electrolytic capacitors will be introduced to LED lighting systems. The lifetime of LED drivers is limited by large electrolytic capacitors. AC LED drivers can directly power LED lamps with an AC source. Given that an AC–DC or DC–DC converter is not required, the size of an LED driver is significantly decreased with high integration and its lifetime is increased. Two conventional AC LED connection structures exist. One is the inverse-parallel connection of two strings of LED directly connected to the AC source. In the other structure, the AC source directly controls the LED string after the bridge rectifier (Fig. 1) [17]. Although no bulky capacitor is found in the rectifier output, both structures exhibit large current distortion and different high peak currents even under the same input voltage and average input current. An AC LED driving circuit controlled in segments was proposed in [18], [19]. This circuit adopts a segmented driving structure to improve the circuit efficiency effectively, reduce the impact of AC source voltage fluctuation on the circuit, and consequently provide an LED with a stable driving current. However, given the stair-like input LED current, its degree of fitting with the input voltage limits the improvement of the power factor (PF) and total harmonic distribution (THD) of this structure. The driving current provided by a direct AC LED driver in [20] can greatly follow the AC source variation. However, the input current is very sensitive to the AC source fluctuation. Considering the traditional reference voltage generated from a resistor string

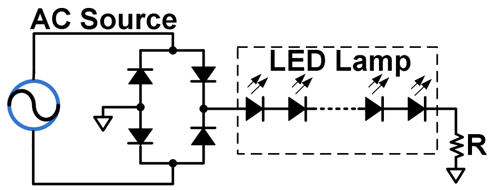

Fig. 1. Bridge AC LED structure.

Manuscript received Nov. 3, 2013; accepted Jan. 3, 2014
Recommended for publication by Associate Editor Sangshin Kwak.
†Corresponding Author: ning_ning@uestc.edu.cn
Tel: +86-28-8320-8233, Fax: +86-28-8320-5248, University of Electronic Science and Technology of China
*State Key Laboratory of Electronic Thin film and Integrated Device, University of Electronic Science and Technology of China, China

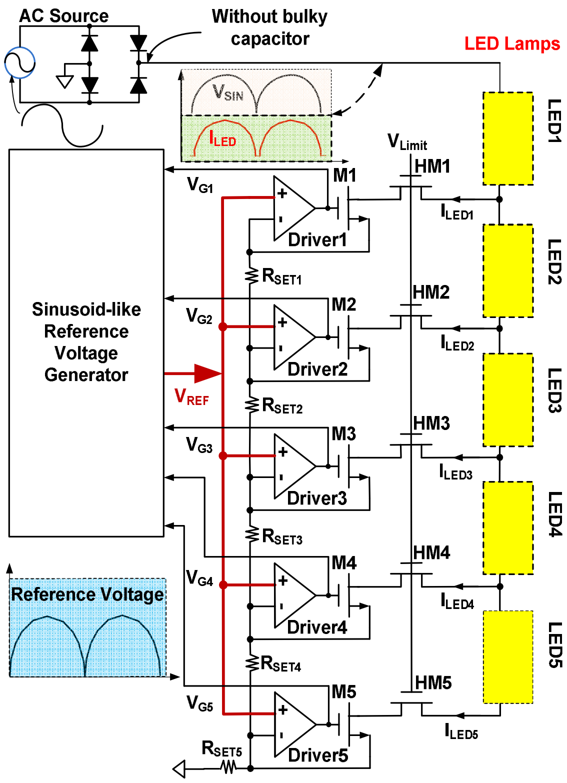

Fig. 2. Architecture of the proposed AC LED driver.

that samples the power supply, the reference voltage encounters fluctuation along the AC source. The stability of the driving current is thus significantly affected. The fluctuation in the driving current upon that of the AC source leads to the instability of LED lamps and creates the feeling that the LED lamp is flashing.

The traditional AC–DC and DC–DC has a low impact on LED brightness. However, LED in normal AC LED is easily influenced by voltage fluctuation. The AC LED proposed in this study can avoid the flash caused by LED current fluctuation, which is in turn generated by an AC source fluctuation. A novel reference voltage generator is applied in this driving structure. Compared with a conventional AC LED driver, this driving circuit provides a stable driving current for LED lamps without the effect of AC voltage fluctuation. At the same time, the high degree of fitting of the driving current waveform with the AC source obtains higher PF and THD in the LED system than the segment-controlled driving structure. The proposed driver, with amendments to the peripheral devices, can be applied to 110 and 220 V AC sources. Therefore, the proposed driver has excellent flexibility. This paper is organized as follows. A specific description of circuit topology is provided in Section 2, and simulation and experimental results are elaborated in Section 3.

II. Architecture of the Proposed LED Driver

A. Block Diagram of the Proposed AC LED Driver

The system block diagram of the proposed AC LED driving circuit is generated in this section. Fig. 2 shows the proposed LED driver. The LED string is connected in series to the output of the bridge rectifier, and the numbers of the input LED string increase along the ascendance of the AC source peak value. A five-string LED was adopted as the lighting unit of the LED system. Drivers 1, 2, 3, 4, and 5 of the driving current units provide the LED lamps with a constant current driver. Every driving current unit includes an operational amplifier (OPA), a current driving MOSFET (Mn), and a resistor soft-switching R_{SETn}. The positive terminals of OPAs are connected to the output of the reference voltage generator, and the negative terminals are connected to the corresponding R_{SETn}. Every driving current unit provides a segmented current for the corresponding LED strings. High-voltage transistors (i.e., $HM1$, 2, 3, 4, and 5) serve as protectors of the driving circuit. The threshold voltage of HMn was set as V_{TH}. When the AC source is extremely high, the output voltage of the driving current unit can only withstand V_{Limit} - V_{TH}, and the extra high voltage is shared with the high-voltage transistor. The reference voltage generator provides the driving current units the reference voltage, which can properly follow the waveform of the AC source and is insensitive to the fluctuation.

The first string of the LED is connected to the output voltage of the bridge rectifier, with the output voltage being V_{SIN}. When V_{SIN} increases from zero to V_{LED1}, the threshold voltage of the first string of the LED, Driver 1, is turned on. The current is then transmitted from resistor R_{STE1} to R_{SET5} by $M1$. At this point, the other four driving current units are closed, and the outputs of the five OPAs (i.e., $V_{G1,2,3,4,5}$) remain at a high level. When V_{SIN} continues to increase to $V_{LED1} + V_{LED2}$, the threshold voltage of the two strings of LED, Driver 2, begins to work and LED1 and LED2 are turned on. The current is transmitted through $M2$ to R_{SET2}, R_{SET3}, R_{SET4}, and R_{SET5}. The current passing through R_{SET1} gradually decreases to zero, and Driver 1 is turned off. The output of OPA1 (V_{G1}) reaches a low level and produces a current that is approximate to zero. This driving structure does not require the use of a switch to control the working state of every driver. On the contrary, automatic switching is implemented. Therefore, no glitch occurs in the switch between every two driving current units. In the same manner, with the increase in V_{SIN}, Drivers 3, 4, and 5 are turned on (in this order). More strings of LED are turned on accordingly. When Drivers 3 and 4 stop working, V_{G3} and V_{G4} drop to a low level, whereas V_{G5} remains high. As V_{SIN} begins to decrease after its peak value, the operating status of the driving current units is symmetrical to the rising period of the voltage. The number of the lighted LED lamp strings decreases with the decrease in V_{SIN}; V_{G4}, V_{G3}, V_{G2}, and V_{G1} increases in order. The segment n current (I_{LEDn}) of the LED lamps provided by every driving current unit is as follows:

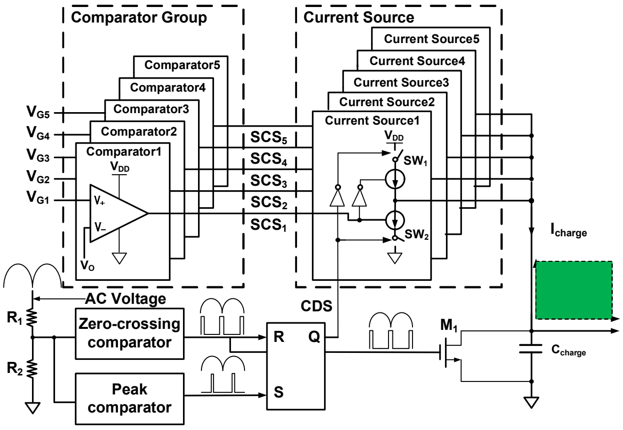

Fig. 3. Structure of the reference voltage generator.

$$I_{LEDn} = V_{REF} \Big/ \sum_{i=n}^{5} R_{SETn} \quad . \qquad (1)$$

Considering that V_{REF} is the reference voltage produced by the reference voltage generator that can closely follow V_{SIN} and is not affected by the AC source, the LED driving current composed of every segmented current can properly fit V_{SIN}; thus, PF and THD are increased. Consequently, users would not feel that LED lamps are flashing when the AC source is unstable.

B. Reference Voltage Generator

As shown in Fig. 3, a novel reference voltage generator was employed in the AC LED driving circuit. The reference voltage (V_{REF}) generated in this structure can well follow the half-sinusoidal waveform. Given that a separated current source exists for the charge and discharge of the capacitor, V_{REF} is insensitive to the tremble of the AC source. The operating principle of this module is discussed in this study.

The input terminals of the zero-crossing and peak comparators are simultaneously connected to the AC line voltage that has been divided by $R1$ and $R2$. The outputs of the zero-crossing and peak comparators are connected to two input terminals of the SR trigger. The output of the SR trigger is connected to selective switches SW_1 and SW_2 as the charge and discharge signal (CDS) of the current source. The zero-crossing comparator produces a transient high pulse when V_{SIN} is zero. Before V_{SIN} increases to the maximum value from zero, the peak comparator and SR trigger outputs remain low. SW_1 is then turned on and SW_2 is turned off. The source current provides the charging current for the capacitor of C_{Charge}, and the capacitor voltage gradually increases from zero. The outputs of the five OPAs (i.e., $V_{G1,\ 2,\ 3,\ 4,\ \text{and}\ 5}$) in the driving current units are connected to the comparator group. As mentioned previously, the increase in V_{SIN}, V_{G1}, V_{G2}, V_{G3}, and V_{G4} turns from high to level in this order, whereas V_{G5} remains high. After going through the comparator group, these gate voltages generate a group of five bit-segmented control signal

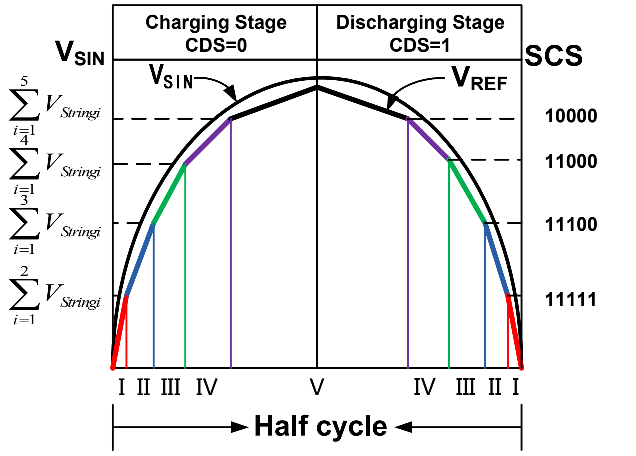

Fig. 4. Illustrative diagram of V_{REF} versus V_{SIN}.

SCS_i (I = 1, 2, 3, 4, 5). When SCS_i is high, current source i is connected to the circuit to provide a charging current for the capacitor. Otherwise, the current source is closed. During the process where V_{SIN} increases from zero to the maximum value, SCS decreases from "11111" to "10000." The total charging current changes along with the change in the V_{SIN} gradient; thus, the output of C_{Charge} closely follows V_{SIN}. When V_{SIN} reaches its maximum value, the peak comparator produces a transient high pulse. The SR trigger generates high voltage accordingly. SW_1 is then turned off and SW_2 is turned on. The current source provides a discharging current for the capacitor C_{Charge}. With the decrease in V_{SIN}, the value of SCS increases and the corresponding discharging current gradually increases. Reset transistor $M1$ prevents the imbalance between charge and discharge of the current source from the voltage shift of the C_{Charge} initial voltage. Therefore, the initial capacitor voltage is zero at the beginning of every cycle.

Fig. 4 is the waveform illustrative diagram of V_{SIN} and V_{REF} derived from AC source after the processing of the bridge rectifier and the reference voltage generator, respectively. We can divide the waveform of the figure into 5 regions. As mentioned before, from regions I to V, CDS is low; C_{Charge} is charging; SCS turns from 11111 to 10000; the total charging current decreases; the corresponding charging voltage gradient also drops. The discharge stage is symmetrical to the charge one. The figure indicates a high fitting degree between the waveform of V_{REF} and that of the V_{SIN}. Considering that the current resource within the chip is directly used to charge the capacitor, V_{REF} is also not sensitive to the AC source fluctuation.

III. Simulated and Experimental Results

A. Simulated Results

The simulation results of the proposed circuit are given in this subsection. The waveform of each part in the reference voltage generator is shown in Fig. 5. Fig. 5(a) demonstrates the waveform of CDS, which controls the charge and discharge of

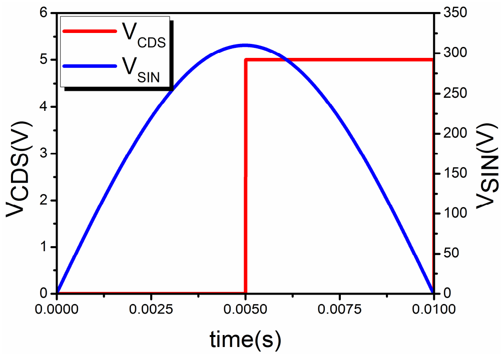

(a) Charge and discharge signal

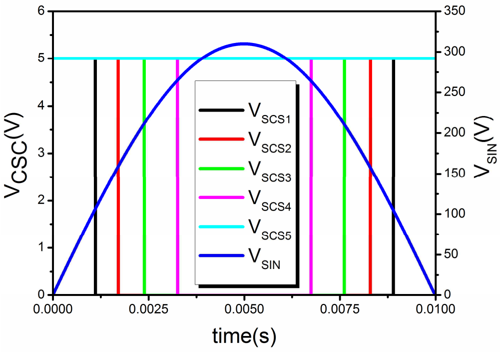

(b) Segmented control signal

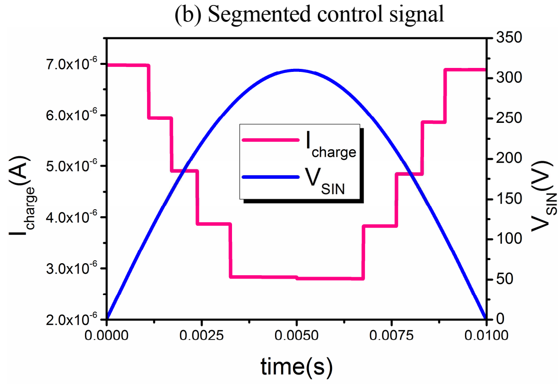

(c) Total charging current

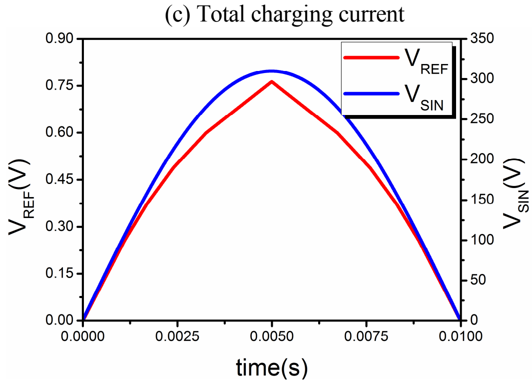

(d) Reference voltage

Fig. 5. Simulated results of the reference voltage generator.

the current source. The change in SCS within a half cycle is shown in Fig. 5(b). Fig. 5(c) provides the total charging current, which is symmetrical to the discharging current. Finally, Fig. 5(c) demonstrates V_{REF}, which is the output voltage of the capacitor C_{Charge}. Its voltage waveform greatly follows the half-sinusoid V_{SIN}.

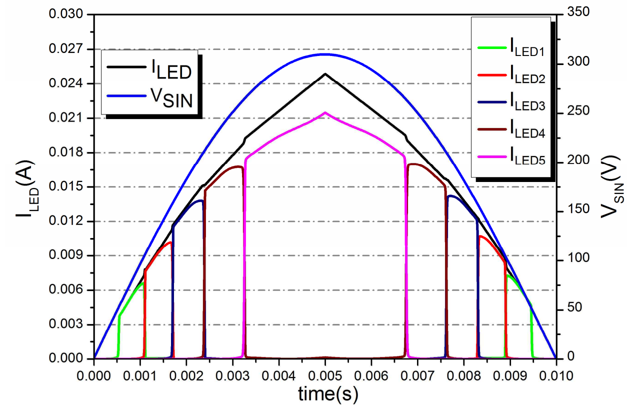

Fig. 6. Simulated I_{LED} versus half-sinusoid V_{SIN} under 220 V at 50 Hz.

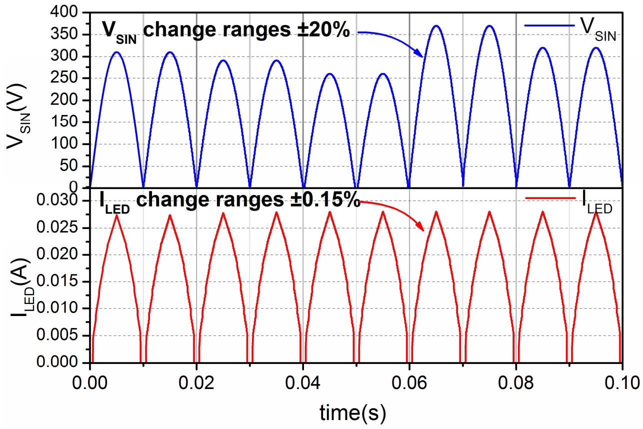

Fig. 7. Simulated I_{LED} versus half-sinusoid V_{SIN} under 220 V at 50 Hz.

The driving current is provided by Drivers 1, 2, 3, 4, and 5 consisting of a five-segment current. The waveform of I_{LED} within the half cycle is shown in Fig. 6. The switching node of every segment current coincides with the charge node of V_{REF}. I_{LED} and V_{SIN} have a high fitting degree. In the simulation, the PF and THD for the five-string 6 W LED load under 220 V at 50 Hz are 0.999 and 3%, respectively. Fig. 7 shows the fluctuation of I_{LED} along V_{SIN} to demonstrate the impact of the AC source on I_{LED}. The maximum value of V_{SIN} is at ± 20%, whereas the fluctuation in I_{LED} is only at ± 0.15%. This result indicates that the driving current is insensitive to the AC source fluctuation.

B. Experiment Results

Fig. 8 shows the measurement result of V_{REF} and V_{SIN} after the rectifier bridge under 220 V at 50 Hz. The measurement result shows that V_{REF} is very close to V_{SIN}. Fig. 9 shows the waveform of driving current I_{LED} and input voltage V_{SIN} after the rectifier bridge. The input current fits input voltage V_{SIN} well. The experiment results indicate that the fluctuation in input voltage V_{SIN} is at ± 10% and the fluctuation in I_{LED} is at ± 0.2%. In comparison with the previous structure, the reference

TABLE I

EXPERIMENTS IN DIFFERENT CONDITIONS

Reference Voltage	Number Of Strings	AC Source	Power	PF	THD
Sinusoid-like Reference	1	220 V	6 W	0.979	20.9%
Sinusoid-like Reference	1	110 V	6 W	0.976	23.4%
Sinusoid-like Reference	5	220 V	6 W	0.999	3.3%
Sinusoid-like Reference	5	110 V	6 W	0.997	6.2%
Stair-like Reference	1	220 V	6 W	0.947	33.9%
Stair-like Reference	5	220 V	6 W	0.997	7.2%

TABLE II

PERFORMANCE COMPARED WITH OTHER REFERENCES

References	PF	THD (%)	Efficiency (%)	Number Of Strings	Power (W)
[12]	0.995	8.6	93.4	6	22
[13]	0.997	7.2	90.2	5	19
This study	0.999	3.3	91.6	5	6

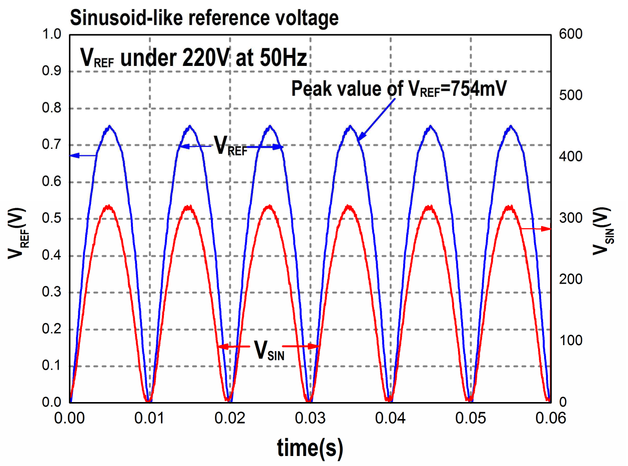

Fig. 8. Measurement result of the sinusoid-like reference voltage under 220 V at 50 Hz.

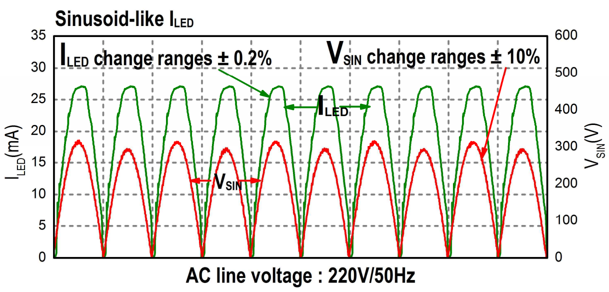

Fig. 9. Measured input voltage and driving current waveform.

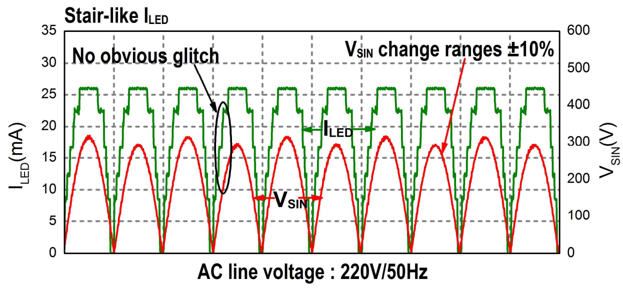

Fig. 10. Measured input voltage and stair-like current waveform.

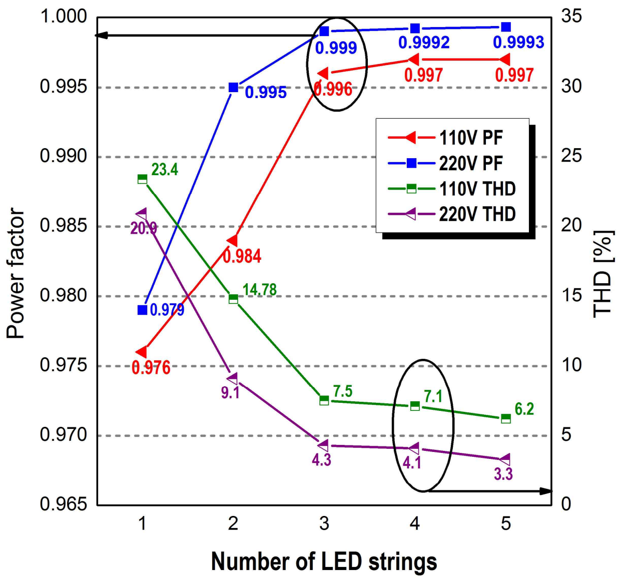

Fig. 11. Power factor and THD versus the number of LED strings. Measurements were conducted at 50 Hz consuming 6 W under different AC supplies.

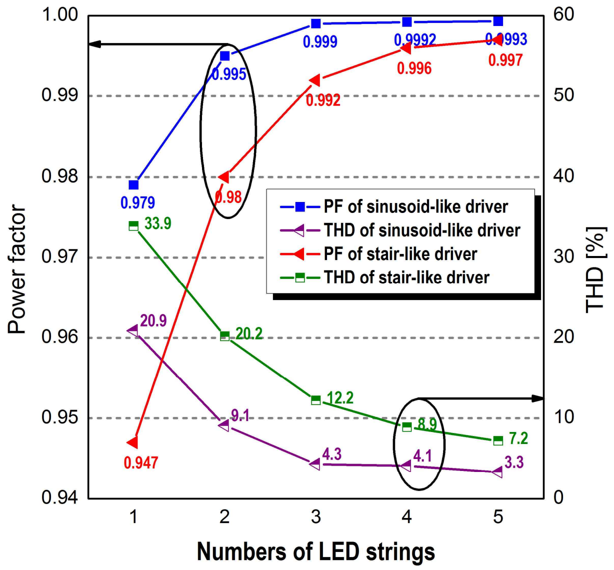

Fig. 12. PF and THD of sinusoid-like and stair-like drivers versus the number of LED strings. Measurements were conducted under 220 V at 50 Hz consuming 6 W.

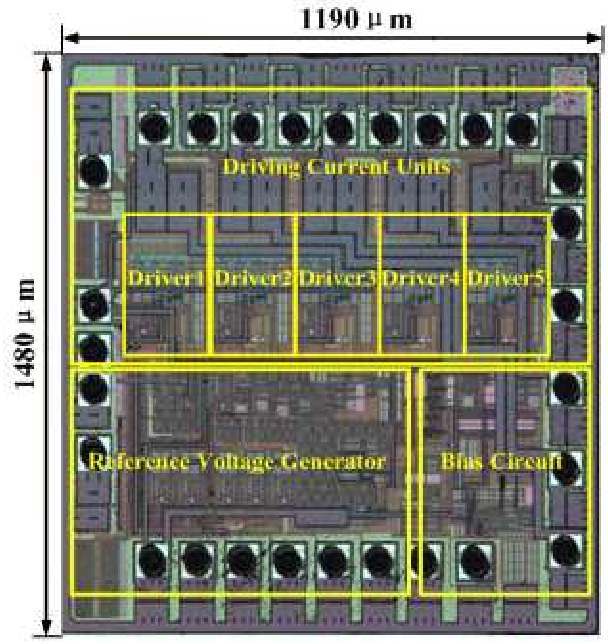

Fig. 13. Micrograph of the fabricated AC LED driver.

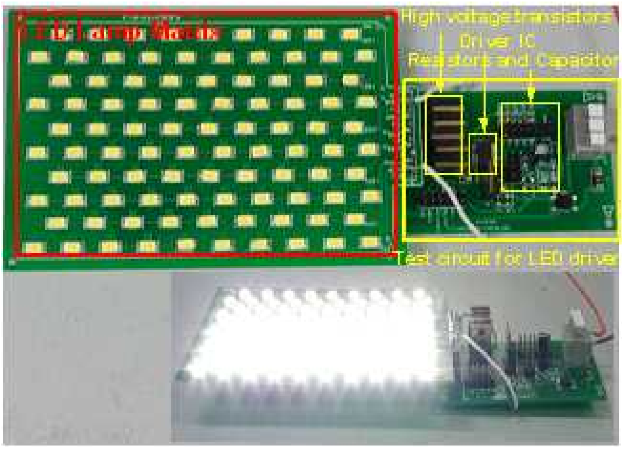

Fig. 14. Photograph of the test circuit with an LED matrix.

of the driving current units was connected to a constant voltage instead of the reference voltage generator. The waveform of the driving current is shown in Fig. 10. The current waveform is in the shape of stairs, and no obvious glitch occurs in the switch between each driving current unit. The measurement results of V_{SIN}, sinusoid-like I_{LED}, and stair-like I_{LED} are obtained under 220 V at 50 Hz consuming 6 W. V_{SIN} changes at ± 10%. Under the same power, the driving current of 110 V is twice that of 220 V. Fig. 11 shows the PF and THD of the sinusoid-like reference-equipped LED driver with different strings. The driver adopts the proposed sinusoid-like reference voltage generator. The achievable PFs are 0.997 and 0.999 for 110 V at 50 Hz and for 220 V at 50 Hz, respectively, with a five-string 6 W LED load. The THDs are 6.2% and 3.3%, respectively. The PFs and THDs for the sinusoid-like and stair-like drivers are provided in Fig. 12. The proposed LED driver using a sinusoid-like reference voltage generator obtains high PF and low THD under the same load. Table I shows PF and THD in different conditions. The experiment results at 220 V/50 Hz and 6 W in this study compared with those in other references are summarized in Table II.

Figs. 13 and 14 show the microphotograph of the fabricated IC and test circuit with an LED lamp matrix. The chip was fabricated through 0.25 μm BCD process, and the die area is 1190 μm × 1480 μm. Given the limitations of the process, the six high-voltage transistors are off-chip. Among the six high-voltage transistors, five were used to protect the driving circuit, and one was used to supply power for the chip. The resistors (i.e., R_{SET1}, R_{SET2}, R_{SET3}, R_{SET4}, and R_{SET5}) were implemented outside the chip so that the driving circuit can be adjusted easily. The values of R_{SET1}, R_{SET2}, R_{SET3}, R_{SET4}, and R_{SET5} are 50, 25, 10, 10, and 30 ohms, respectively. Instead of being integrated, the resistors are out-of-chip; therefore, the heating problem of the resistors can be effectively controlled. The charge capacitor was also placed off-chip to obtain a more accurate V_{REF} value.

IV. CONCLUSIONS

An AC LED driver with a sinusoid-like reference and highly resistant to AC voltage fluctuation was developed. The absence of passive components significantly improved the stability and integration of the LED system. The driving circuit of this structure allows the input current of LED to follow the waveform of the input voltage properly; thus, PF is increased and THD is decreased. The driving circuit is also insensitive to AC voltage fluctuation. As a result, users would not feel that LED lamps are flashing during input voltage fluctuation. The proposed driver, with amendments to the peripheral devices, can be applied to 110 and 220 V AC sources and thus has excellent flexibility. This suitability of this driver was demonstrated by a prototype implementation in a 0.25 μm BCD process. The PF and THD of the driving circuit under 6 W/110 V and 6 W/220 V AC voltage reached 0.997/0.999 and 6.2%/3.3%, respectively. The efficiencies are 90.3% and 91.6% for 110 V at 50 Hz and for 220 V at 50 Hz, respectively, with a power consumption of 6 W.

ACKNOWLEDGMENT

This work was supported by the Fundamental Research Funds for Central Universities under project no. ZYGX2012Z007.

REFERENCES

[1] J. Y. Tsao, "Solid-state lighting: lamps, chips, and materials for tomorrow," *IEEE Circuits Devices Mag.*, Vol. 20, No. 3, pp. 28-37, May/Jun. 2004.

[2] N. Narendran and Y. Gu, "life of LED-based white light sources," *J. Display Technol.*, Vol. 1, No. 1, pp. 167-171, Sep. 2005.
[3] M. S. Shur and R. Zukauskas, "Solid-state lighting: toward superior illumination," in *Proc. IEEE*, Vol. 93, No. 10, pp. 1691-1703, 2005
[4] J. Brodrick, "Next-generation lighting initiative at the U.S. department of energy catalyzing science into the marketplace," *J. Display Technol.*, Vol. 3, No. 2, pp. 91-97, Jun. 2007.
[5] Y. K. Cheng and K. W. E. Cheng, "General study for using LED to replace traditional lighting devices," in *Proc. 2nd Int. Conf. Power Electron. Syst. Appl.*, pp. 173-177, 2006.
[6] F. Xiaoyun, L. Xiaojian, and W. Yan, "Research and analysis of the design development and perspective technology for LED lighting products," in *Proc. IEEE Comput.-Aided Ind. Design Conceptual Design*, pp. 1330–1334, Nov. 2009.
[7] L. Yu and J. Yang, "The topologies of white LED lamp's power drivers," in *Proc. IEEE PESA,* pp. 1-6, 2009.
[8] K.. I. Hwu and Sheng-Chien Chou, "A simple current-balancing converter for LED lighting," in *Proc. IEEE APEC,* pp. 587-590, 2009.
[9] Y. K. Cheng and K. W. E. Cheng, "General study for using LED to replace traditional lighing devices," in *Proc. IEEE ICPESA*, pp. 173-177, 2006.
[10] K. Zhou, J. Z. Guo, S. Yuvarajan and D. F. Weng, "Quasiactive power factor correction circuit for HB LED driver," *IEEE Trans. Power Electron.*, Vol. 23, No. 3, pp. 1410-1415, May 2008.
[11] Y. C. Chuang, Y. L. Ke, H. S. Chuang and C. C. Hu "Single-stage power-factor-correction circuit with flyback converter to drive LEDs for lighting applications," in *Proc. IEEE IAS.*, pp. 1-9, 2010.
[12] J. M. Alonso, J. Vina, D. G. Vaquero, G. Martinez and O. Rene, "Analysis and design of the integrated double buck-boost converter as a high-power-factor driver for power-LED lamps," *IEEE Trans. Ind. Electron.*, Vol. 59, No. 4, pp. 1689-1697, Apr. 2012.
[13] Y. Hu, L. Huber, and M. M. Jovanović, "Single-stage, universal-input AC/DC LED driver with current- controlled variable PFC boost inductor," *IEEE Trans. Power Electron.*, Vol. 27, No. 3, pp. 1579-1588, Mar. 2012.
[14] D. G. Lamar, J. Sebastian, M. Arias, and M. M. Hernando, "A low-cost ac–dc high-brightness LED driver with power factor correction based on standard peak-current mode integrated controllers," in *Proc. IEEE Energy Convers. Congr. Expo.*, pp. 463-470, 2010.
[15] Y. C. Li and C. L. Chen, "A novel single-stage high-power-factor AC-to-DC LED driving circuit with leakage inductance energy recycling," *IEEE Trans. Ind. Electron.*, Vol. 59, No. 2, pp. 793-802, Feb. 2012.
[16] Z. Ye, F. Greenfeld, and Z. Liang, "A topology study of single-phase offline ac/dc converters for high brightness white LED lighting with power factor pre-regulation and brightness dimmable," in *Proc. 34th IEEE Annu. Conf. Ind. Electron.* , pp. 1961–1967, 2008.
[17] M. Miskin, J.N. Anderson, "AC light emitting diode and AC LED drive methods and apparatus," *U.S. PAT. No. 20070273299.*
[18] J. Kim, J. Lee, S. Park, "A Soft Self-Commutating Method Using Minimum Control Circuitry for Multiple-String LED Drivers," in *Proc. Int. Solid State Circuits Conf.*, pp. 376–377, 2013.
[19] N. Ning, W. B. Chen, D. J. Yu, C. Y. Feng and C. B. Wang, "A self-adaptive load technology for AC multiple-string LED drivers," *IEEE Electronics Letters*, Vol. 49, pp. 1170-1171, Aug. 2013.
[20] Dayal, R., Modepalli, K. and Parsa, L., "A direct AC LED driver with high power factor without the use of passive components," in *Proc. IEEE Energy Convers. Cong. Expo.*, pp. 4230-4234, 2012.

Ning Ning received his B.S. and Ph.D. degrees from the University of Electronic Science and Technology of China, Chengdu, China, in 2002 and 2007, respectively. Since 2007, he has been with the State Key Lab of Electronic Thin Films and Integrated Devices, University of Electronic Science and Technology of China, where he is now an associate professor. His current research interests include power electronics as well as analog and mixed-signal IC design.

Zhenxiao Tong received his B.S. degree from the University of Electronic Science and Technology of China, Chengdu, China, in 2011. He is currently pursuing his M.S. degree from the University of Electronic Science and Technology of China, Chengdu, China. His current research interests include power electronics and analog IC design.

Dejun Yu received his B.S. and M.S. degrees from the University of Electronic Science and Technology of China, Chengdu, China, in 2002 and 2006, respectively. He worked at Eutech Microelectronics Inc., Chengdu, China, from 2006 to 2012. He is currently pursuing his Ph.D. degree at the University of Electronic Science and Technology of China, Chengdu, China. His current research interests include power management and signal processing techniques.

Shuangyi Wu received his B.S. and M.S. degrees from the University of Electronic Science and Technology of China, Chengdu, China, in 2004 and 2007, respectively. He worked as a senior engineer at Sunplus Technology Co., Ltd., Chengdu, China, from 2007 to 2011. He is currently pursuing his Ph.D. degree at the University of Electronic Science and Technology of China, Chengdu, China. His current research interests include signal processing techniques as well as analog and mixed-signal IC design.

Wenbin Chen received his B.S. degree from Southwest Jiaotong University, Chengdu, China, in 2011. He is currently pursuing his M.S. degree at the University of Electronic Science and Technology of China, Chengdu, China. His current research interests include power electronics and analog IC design.

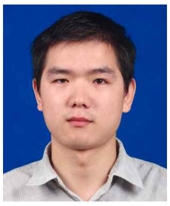

Chunyi Feng received his B.S. and M.S. degrees from the University of Electronic Science and Technology of China, Chengdu, China, in 2010 and 2013, respectively. He is currently working at JAVEE Microelectronics, Inc., Chengdu, China. His interests include power electronics and analog IC design.